The Astrophysical Journal, 790:38 (10pp), 2014 July 20 doi:10.1088/0004-637X/790/1/38

ON THE RADIOLYSIS OF ETHYLENE ICES BY ENERGETIC ELECTRONS AND IMPLICATIONS TO THE EXTRATERRESTRIAL HYDROCARBON CHEMISTRY

Li Zhou[1], Surajit Maity[2], Matt Abplanalp[2], Andrew Turner[2], and Ralf I. Kaiser[2]
[1] Department of Chemistry, Nanchang University, Nanchang 330031, China
[2] Department of Chemistry, University of Hawaii at Manoa, Honolulu, HI 96822, USA; ralfk@hawaii.edu
Received 2013 October 23; accepted 2014 April 29; published 2014 July 1

ABSTRACT

The chemical processing of ethylene ices (C_2H_4) by energetic electrons was investigated at 11 K to simulate the energy transfer processes and synthesis of new molecules induced by secondary electrons generated in the track of galactic cosmic ray particles. A combination of Fourier transform infrared spectrometry (solid state) and quadrupole mass spectrometry (gas phase) resulted in the identification of six hydrocarbon molecules: methane (CH_4), the C2 species acetylene (C_2H_2), ethane (C_2H_6), the ethyl radical (C_2H_5), and—for the very first time in ethylene irradiation experiments—the C4 hydrocarbons 1-butene (C_4H_8) and n-butane (C_4H_{10}). By tracing the temporal evolution of the newly formed molecules spectroscopically online and in situ, we were also able to fit the kinetic profiles with a system of coupled differential equations, eventually providing mechanistic information, reaction pathways, and rate constants on the radiolysis of ethylene ices and the inherent formation of smaller (C1) and more complex (C2, C4) hydrocarbons involving carbon–hydrogen bond ruptures, atomic hydrogen addition processes, and radical–radical recombination pathways. We also discuss the implications of these results on the hydrocarbon chemistry on Titan's surface and on ice-coated, methane-bearing interstellar grains as present in cold molecular clouds such as TMC-1.

Key words: astrochemistry – methods: laboratory: solid state – molecular processes – planets and satellites: individual (Titan) – radiation: dynamics

Online-only material: color figures

1. INTRODUCTION

Titan's similarity to Earth such as a dense atmosphere and richness of nitrogen has stirred considerable interest from the planetary science and astrochemistry communities over the past few decades. Titan's surface pressure and temperature have been determined to be 1.4 bar and 94 K, respectively (Raulin 2005; Lunine & Lorenz 2009). Nitrogen (98.4%) and methane (1.6%), as well as trace hydrocarbons (acetylene (C_2H_2), ethylene (C_2H_4), ethane (C_2H_6), methylacetylene (CH_3CCH), propane (C_3H_8), diacetylene (C_4H_2), benzene (C_6H_6)), nitriles (hydrogen cyanide (HCN), cyanoacetylene (HCCCN), cyanogen (C_2N_2)), and oxygen-bearing molecules (carbon dioxide (CO_2), carbon monoxide (CO), water (H_2O)) constitute Titan's atmosphere (Coustenis et al. 2003, 2007; Niemann et al. 2005; Vinatier et al. 2007). In its upper layers, Titan's complex chemistry is triggered by solar photons and energetic electrons; this results in fast ion–molecule and neutral–neutral reactions forming complex molecules such as nitriles (Zhang et al. 2009a; Kaiser & Mebel 2012), polyynes (Gu et al. 2009; Zhang et al. 2009b; Jones et al. 2011; Dangi et al. 2013) and even polycyclic aromatic hydrocarbons (PAHs) such as naphthalene (Parker et al. 2012; Kaiser et al. 2012). These molecules might agglomerate (Sigurbjornsson & Signorell 2008) or sequester onto Titan's surface (Zhou et al. 2008; Tomasko et al. 2009).

As early as 1984, Sagan & Thompson (1984) pointed out that energetic galactic cosmic ray (GCR) particles could penetrate deep into the lower atmospheric layers, pass their kinetic energy to simple organics in Titan's lower atmosphere, and also induce nonequilibrium chemical reactions within surface solids. Consequently, it is important to probe the interaction of ionizing radiation with abundant organic molecules such as methane (Bennett et al. 2006), ethane (Kim et al. 2010), and nitriles on Titan's surface. Here we select energetic electrons as generated in the track of high energy GCRs as a radiation source. In 1999, Molina-Cubero et al. (1999) quantified the energy deposition on Titan's surface by GCRs to be 4.5×10^7 eV cm^{-2} s^{-1}. However, the radiation processing of simple organics on Titan's surface—with the exception of acetylene (C_2H_2; Zhou et al. 2010) and ethane (C_2H_6; Kim et al. 2010)—by energetic electrons is not well understood. In order to gain a comprehensive picture of the hydrocarbon chemistry and to fill the gap between the hydrogen-rich (ethane (C_2H_6)) and hydrogen-poor (acetylene (C_2H_2)) ices studied earlier in our laboratory, we report here the radiation-induced chemistry of low temperature ethylene (C_2H_4) ices by energetic electrons as generated in the track of GCR particles.

2. EXPERIMENTAL

The experiments were carried out in a contamination-free ultrahigh vacuum (UHV) chamber (5×10^{-11} torr; Bennett et al. 2004). A silver wafer, which acts as a substrate, is located in the center of the chamber and cooled by a closed cycle helium refrigerator to 11.0 ± 0.3 K. Ethylene (C_2H_4) ices with a thickness of 500 ± 200 nm were prepared after depositing gaseous ethylene (99.999%, Linde) through a glass capillary array for three minutes at a pressure of 1×10^{-7} torr. We utilize a Thermo Nicolet 6700 Fourier transform infrared (FTIR) spectrometer and a quadrupole mass spectrometer (Balzer QMG 420) to probe molecules in the condensed phase and in the gas phase, respectively. Figure 1 depicts the mid-infrared spectra of the ethylene ice recorded immediately after the deposition at 11 K, along with assignments (Table 1). The FTIR spectrometer monitors the modification of the ices online and in situ from 6000 to 400 cm^{-1} at a resolution of 4 cm^{-1}, while the quadrupole

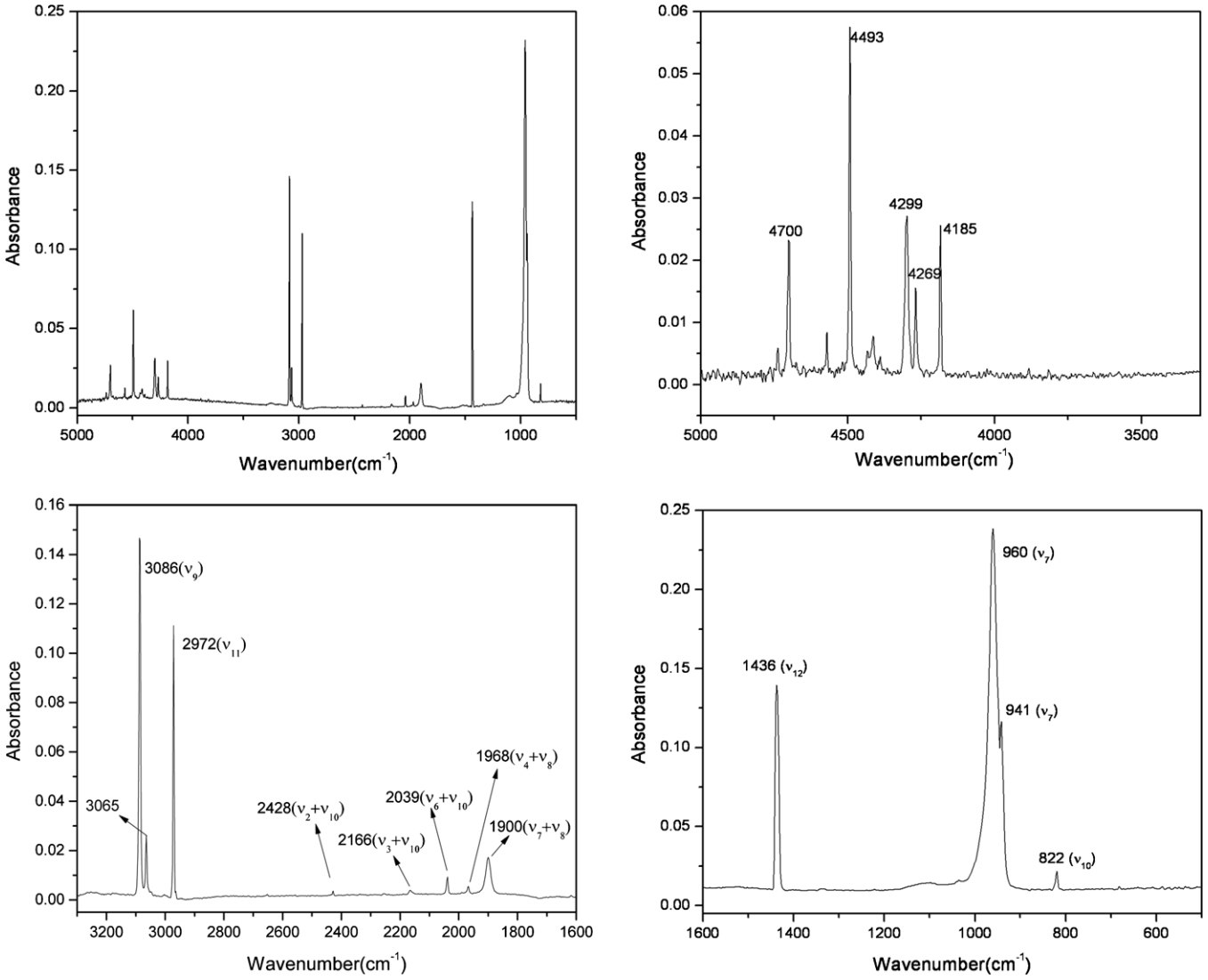

Figure 1. Infrared spectra of solid ethylene ice (C_2H_4) before the irradiation at 11 K. The upper left spectra shows the complete spectral range from 5000 to 400 cm^{-1}, whereas the remaining three panels present zoomed regions.

Table 1
Assignments of the Vibrational Modes of the Ethylene (C_2H_4) Ices at 11 K

Absorption (cm^{-1})	Literature Value[a] (cm^{-1})	Assignment	Carrier
4700, 4493, 4299, 4269, 4185	...	...	...
3086	3075	ν_9	CH_2 asym.str.
2972	2973	ν_{11}	C-H str.
2428	2434	$\nu_2 + \nu_{10}$	...
2166	2166	$\nu 3 + \nu_{10}$	...
2039	2043	$\nu_6 + \nu_{10}$	...
1968	1969	$\nu_4 + \nu_8$	...
1900	1902	$\nu_7 + \nu_8$	...
1436	1436, 1440	ν_{12}	CH_2 scissor
960, 941	970	ν_7	CH_2 wag
822	826, 828	ν_{10}	CH_2 rock

Note. [a] Brecher & Halford (1961).

mass spectrometer (QMS) operates in residual gas analyzer mode with an electron impact ionization energy of 90 eV and an emission current of 2 mA to detect the subliming species in the follow-up warming process. The ices were irradiated with 5 keV electrons at a nominal beam current of 0 nA (control experiment) and 1000 nA at 11 K for 60 minutes. The electron beam was generated using an electron source (Specs EQ 22–35) and scanning the beam over the target area of 3.2 ± 0.3 cm^2. Since the extraction efficiency of the electron gun is 78.8%, this led to a deposition of 5.5 × 10^{15} electrons cm^{-2} into the ethylene ices. After the irradiation, the samples were kept at 11 K for 1 hr and were then heated to 300 K at 0.5 K $minute^{-1}$. The energy deposition by the electrons was explored and simulated by the CASINO code (Drouin et al. 2001), yielding an average absorbed dose of 37 ± 8 eV $molecule^{-1}$.

The thickness of the sample was determined in situ using laser interferometry. Here the cooled silver target is rotated to face two HeNe lasers (632.8 or 543.5 nm). The laser light strikes the target at incident angles of 10°.1 and 11°.5, respectively, relative to the sample normal and is reflected toward two photodiodes with narrow bandpass filters. For each laser, the induced current in the photodiode is monitored as a function of time with a picoammeter, while the gas is introduced into the chamber at

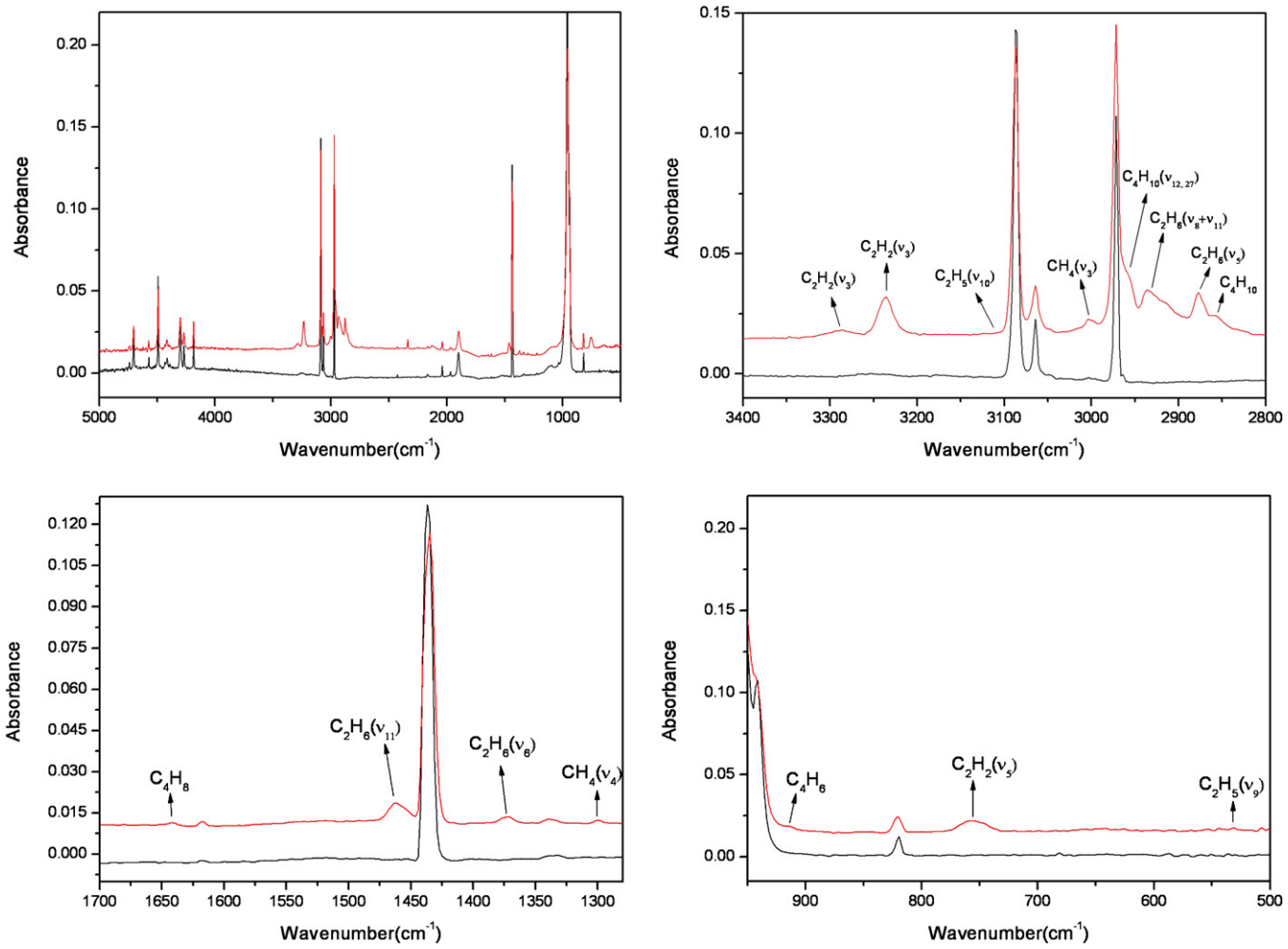

Figure 2. Infrared spectra of the solid ethylene ice (C_2H_4) together with the assignment of newly formed molecules before (black) and after (red) the irradiation. The upper left panel shows the complete spectral range from 5000 to 400 cm^{-1}, whereas the remaining three panels present zoomed regions.
(A color version of this figure is available in the online journal.)

a constant rate through a precision leak valve, whereupon it is condensed onto the low temperature silver target. During the deposition, the HeNe laser is reflected off the surface of the silver target and the freshly deposited ice sample, causing an interference pattern. The period of the interference curve between two maxima or minima relates to a change in thickness as described by Heavens (1965). Here a priori knowledge is required of the index of refraction of ethylene (1.33) for the determination of the deposited ice thickness.

3. RESULTS

3.1. Infrared Spectroscopy

First, we would like to discuss the novel absorption features arising during the irradiation (Figure 2) and aim to assign their carriers. Figure 2 compares the infrared spectra of ethylene at 11 K before and after the irradiation. The newly emerging features and their assignments are compiled in Tables 2 and 3. We identified six new molecules: acetylene (C_2H_2), ethane (C_2H_6), methane (CH_4), n-butane (C_4H_{10}), 1-butene (C_4H_8), and the ethyl radical (C_2H_5). In detail, fundamentals of acetylene were detected at 3286 and 757 cm^{-1} (Bennett et al. 2006). Methane absorptions were monitored at 3003 cm^{-1} and 1300 cm^{-1}, which are in excellent agreement with the data reported earlier (Moore & Hudson 2003; Bennett et al. 2006). The weak absorptions of the ethyl radical were identified via its 532 cm^{-1} and 3110 cm^{-1} absorption bands (Bennett et al. 2006; Pacansky & Schrader 1983). Ethane (C_2H_6) and n-butane (C_4H_{10}) are tricky to discriminate since their most intense features at 2935, 2879, 1462, and 1373 cm^{-1} can be assigned to either molecule (Comeford & Gould 1960; Kim et al. 2010). However, the newly emerging absorptions at 2957 cm^{-1} and 2858 cm^{-1} can be attributed to n-butane. Furthermore, the 2737 cm^{-1} and 2727 cm^{-1} absorptions can be linked to the combination band of ethane (C_2H_6; Kim et al. 2010). To provide further evidence of ethane and n-butane production, we sublimed the newly formed molecules by heating the target to 300 K. Kim et al. (2010) demonstrated that ethane (C_2H_6) sublimes at 60–70 K, while the heavier n-butane (C_4H_{10}) still remains on the target at that temperature. A comparison of the infrared spectra at 11 K and 90 K (Figure 3; Table 4) depicts a substantial decrease in the intensity of the absorptions at 2935, 2879, 1462, and 1373 cm^{-1}, implying complete sublimation of ethane (C_2H_6) into the gas phase. Furthermore, the infrared spectrum at 90 K depicts absorptions at 2962, 2932, 2873, 1461, 1378, and 953 cm^{-1} that can be linked to n-butane (Kim et al. 2010). Finally, the 1642 cm^{-1}, 995 cm^{-1}, and 912 cm^{-1} absorptions can be assigned to the C=C stretch and the $=CH_2$ wag modes of 1-butene (C_4H_8; Comeford & Gould 1960).

Table 2
Infrared Absorption Features of the Newly Formed Species in Irradiated Ethylene (C_2H_4) Ices at 11 K

Absorption (cm^{-1})	Literature Value (cm^{-1})	Assignment	Carrier
3286 (m)	3261	ν_3 C_2H_2	...
3236 (s)	...	ν_3 C_2H_2	C(sp)-H stretch
3110 (w)	3112[a], 3108	ν_{10} C_2H_5	CH_2 asym str.
3003	3001, 3005 (3011[b])	ν_3 CH_4	...
2957	2957	ν_{12}, ν_{27} C_4H_{10}	CH_3 str
2935 (s)	2942	ν_8 + $\nu_{11}C_2H_6$ or ν_{13} C_4H_{10}[c]	Combination (CH_2 asym str C_4H_{10})
2879(s)	2880	ν_5 C_2H_6 or ν_{28} C_4H_{10}[c]	CH_3 stretch
2858	2860	C_4H_{10}[c]	CH_2 sym str.
2737 2727	2736	ν_2 + ν_6 C_2H_6	Combination
2132 2120	...	...	C_2H_2; C = C
1642	1645	C_4H_8	(C = C stretch)
1462(s)	1462	ν_{11} C_2H_6 or ν_{14}, ν_{30}, ν_{31} C_4H_{10}[c]	CH_3 deform
1373	1369	ν_6 C_2H_6 or ν_{32} C_4H_{10}[c]	CH_3 deform
1300	1298	ν_4 CH_4	Deform
913(w)	911	C_4H_6 or C_4H_8[c]	
757(s)	735	ν_5 C_2H_2	CCH bend
532	534	ν_9 C_2H_5	

Notes.
[a] Pacansky & Schrader (1983).
[b] Moore & Hudson (2003).
[c] Kim et al. (2010).

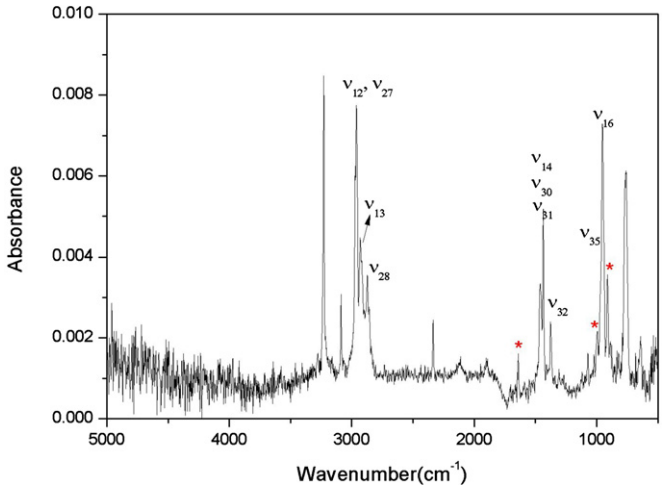

Figure 3. Infrared spectra of the irradiated ethylene ices warmed up to 90 K. The assignments of n-butane (C_4H_{10}) are compiled in Table 4. A set of red asterisks are marked for 1-butene (C_4H_8).
(A color version of this figure is available in the online journal.)

3.2. Mass Spectroscopy

In addition to the in situ infrared analysis, our experimental setup also permits the observation of the products subliming into the gas phase by utilizing a quadrupole mass spectrometer (QMS) during the warm-up phase (Figure 4). The QMS ion currents of the alkanes, methane (CH_4; $m/z = 16$), ethane (C_2H_6; $m/z = 30$), and n-butane (C_4H_{10}; $m/z = 58$), are clearly visible and cannot result from dissociative fragmentation of any higher hydrocarbon upon ionization. However, note that dissociative ionization and the formation of smaller fragment ions is always a byproduct of electron impact ionization with 90 eV electrons. For instance, ions at $m/z = 56$ could originate from ionized 1-butene (C_4H_8) but also from dissociative ionization of the n-butane (C_4H_{10}; $m/z = 58$) parent to $m/z = 56$. A closer look at the temperature-dependent profiles of $m/z = 58$ and 56 indicates that both plots do not overlap, suggesting that the additional ion counts at $m/z = 56$, which are visible from 150 K to 200 K, might originate from 1-butene (C_4H_8). On the other hand, the profiles of the ion currents of $m/z = 56$ and 54 are similar, suggesting that the signal at $m/z = 54$ arises from dissociative ionization of butene (C_4H_8) and that no molecule with the molecular formula C_4H_6 is formed.

4. DISCUSSION

On the basis of the infrared assignments of the newly formed species and the extracted column densities (Figure 5), we are now proposing the underlying formation mechanisms of the molecules synthesized during the irradiation exposure of ethylene ices. For this, we developed a kinetic reaction scheme (Figure 6) and fit the temporal evolution of the column densities via a set of coupled differential equations. The analysis of the derived rate constants indicates that ethylene (C_2H_4) undergoes radiolysis to form acetylene (C_2H_2) via the elimination of two hydrogen atoms and/or molecular hydrogen. This process is associated with a rate constant k_1 of $1.3 \pm 0.2 \times 10^{-5}$ s^{-1}. The competing hydrogen atom addition leading to the ethyl

Table 3
Compilation of New Molecules Found After the Irradiation of Ethylene (C_2H_4) Ices at 11 K

Molecule	Absorption (cm^{-1})	Literature Value (cm^{-1})	Assignment
C_2H_2	3286	3263[a], 3267[b]	ν_3
	3236	...	ν_3
	757	746[a], 761[c]	ν_5
C_2H_6	2935	2941[a], 2942[d]	$\nu_8 + \nu_{11}$
	2879	2879[a], 2880[d]	ν_5
	1462	1464[a], 1462[d]	ν_{11}
	1373	1370[a], 1369[d]	ν_6
	2737, 2727	2736[a]	$\nu_2 + \nu_6$
C_4H_{10}	2935	2926[a], 2930[d]	ν_{13}
	2879	2872[a], 2870[d]	ν_{28}
	1462	1458[a], 1461[d]	$\nu_{14}, \nu_{30}, \nu_{31}$
	1373	1374[a], 1379[d]	ν_{32}
	2957	2958[a], 2968[d]	ν_{12}, ν_{27}
	2858	2859[a]	ν_5
CH_4	3003	3008[a], 3011[e]	ν_3
	1300	1300[a], 1298[e]	ν_4
C_4H_8	1642	1643[a], 1645[d]	C = C stretch
	912	911[a], 910[d]	$=CH_2$ wag
C_4H_6	913	911[a]	...
C_2H_5	3110	3108[a], 3112[f]	ν_{10}
	532	532[a], 540[f]	ν_9

Notes.
[a] Pacansky & Schrader (1983).
[b] Moore & Hudson (2003).
[c] Kim et al. (2010).
[d] Bennett et al. (2006).
[e] Coustenis et al. (1999).
[f] Comeford & Gould (1960).

Table 4
Assignments of Absorptions of n-butane (C_4H_{10}) and 1-butene (C_4H_8) at 90 K After Sublimation of Ethane (C_2H_6) Products

	Absorption (cm^{-1})	Literature Value (cm^{-1})	Assignment	Carrier
C_4H_{10}	2962	2968[a]	ν_{12}, ν_{27}	CH_3 asym stretch
	2932	2930[a]	ν_{13}	CH_2 asym stretch
	2873	2870[b]	ν_{28}	CH_3 sym stretch
	1461	1461[a]	$\nu_{14}, \nu_{30}, \nu_{31}$	CH_3/CH_2 bend
	1378	1379[a]	ν_{32}	CH_3 deform
	953	948[a]	ν_{16}	CH_3 rock
C_4H_8	1642	1643[c]	...	C = C stretch
	995	993[c]	...	HC = CH wag
	912	911[c]	...	$=CH_2$ wag

Notes.
[a] Pacansky & Schrader (1983).
[b] Moore & Hudson (2003).
[c] Kim et al. (2010).

radical (C_2H_5; $k_3 = 3.3 \pm 0.4 \times 10^{-6}$ s^{-1}) is less competitive. It should be noted that at least on the basis of the derived reaction pathways, suprathermal hydrogen atoms do not add to the ethylene molecule. The fits suggest that an ethylene dimer complex undergoes an intramolecular hydrogen transfer to an ethyl (C_2H_5) radical plus a vinyl radical (C_2H_3). Intramolecular hydrogen transfer processes are initiated in dimers of, for instance, hydrocarbons like diacetylene ($(C_4H_2)_2$) upon photolysis at Lyα (Huang et al. 2010). A second hydrogen transfer reduces the ethyl (C_2H_5) radical to ethane (C_2H_6; $k_4 = 1.2 \pm 0.2 \times 10^{-3}$ s^{-1}). The faster rate constant compared with k_3 can be rationalized on the basis of the open-shell structure of the ethyl radical (barrier-less addition of hydrogen) compared with a barrier for the addition to ethylene. The synthesis of methane (CH_4) was also observed in the radiolysis of ethane (C_2H_6) studied previously in our laboratory (Kim et al. 2010). In both systems, ethane decomposed via retro-carbene (CH_2) insertion to form methane plus singlet carbene ($k_8 = 1.2 \pm 0.3 \times 10^{-3}$ s^{-1}). The decomposition of ethylene—possibly via methylcarbene ($HCCH_3$) and carbon retro-insertion (Kaiser & Roessler 1998)—presents a minor pathway ($k_9 = 1.3 \pm 0.1 \times 10^{-5}$ s^{-1}). Carbene (CH_2) was proposed to react with atomic hydrogen recycling methane (CH_4; $k_{11} = 1.2 \pm 0.2 \times 10^{-3}$ s^{-1}). Now our attention is on the newly observed C4 hydrocarbons 1-butene (C_4H_8) and butane (C_4H_{10}). Here a barrier-less radical–radical reaction between two ethyl radicals (C_2H_5) leads to the formation of n-butane ($k_5 = 3.0 \pm 0.4 \times 10^{-20}$ cm^2 $molecule^{-1}$ s^{-1}). Note that the infrared spectra explicitly determine the existence of the n-butane ($CH_3CH_2CH_2CH_3$) isomer but not of the branched isobutane isomer ($(CH_3)_2CHCH_3$); the formation of n-butane can be easily explained via the recombination of two ethyl radicals. Furthermore, radiolyzed n-butane undergoes hydrogen elimination to 1-butene ($k_6 = 1.7 \pm 0.2 \times 10^{-4}$ s^{-1}). A second pathway to 1-butene involves the formal

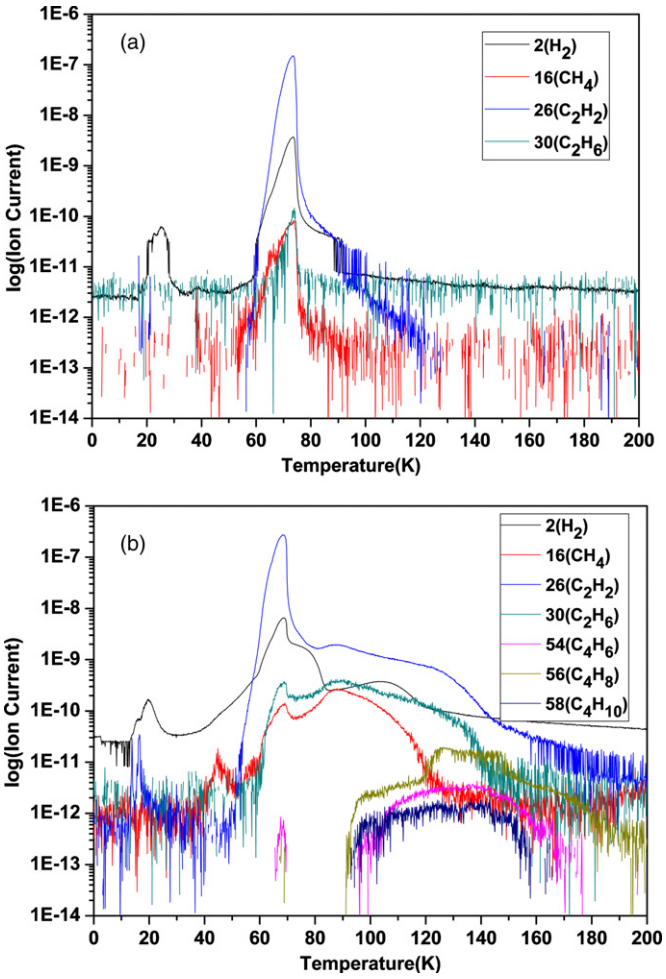

Figure 4. QMS traces of selected ion currents for two sets of experiments: (a) 0 nA and (b) 1000 nA.
(A color version of this figure is available in the online journal.)

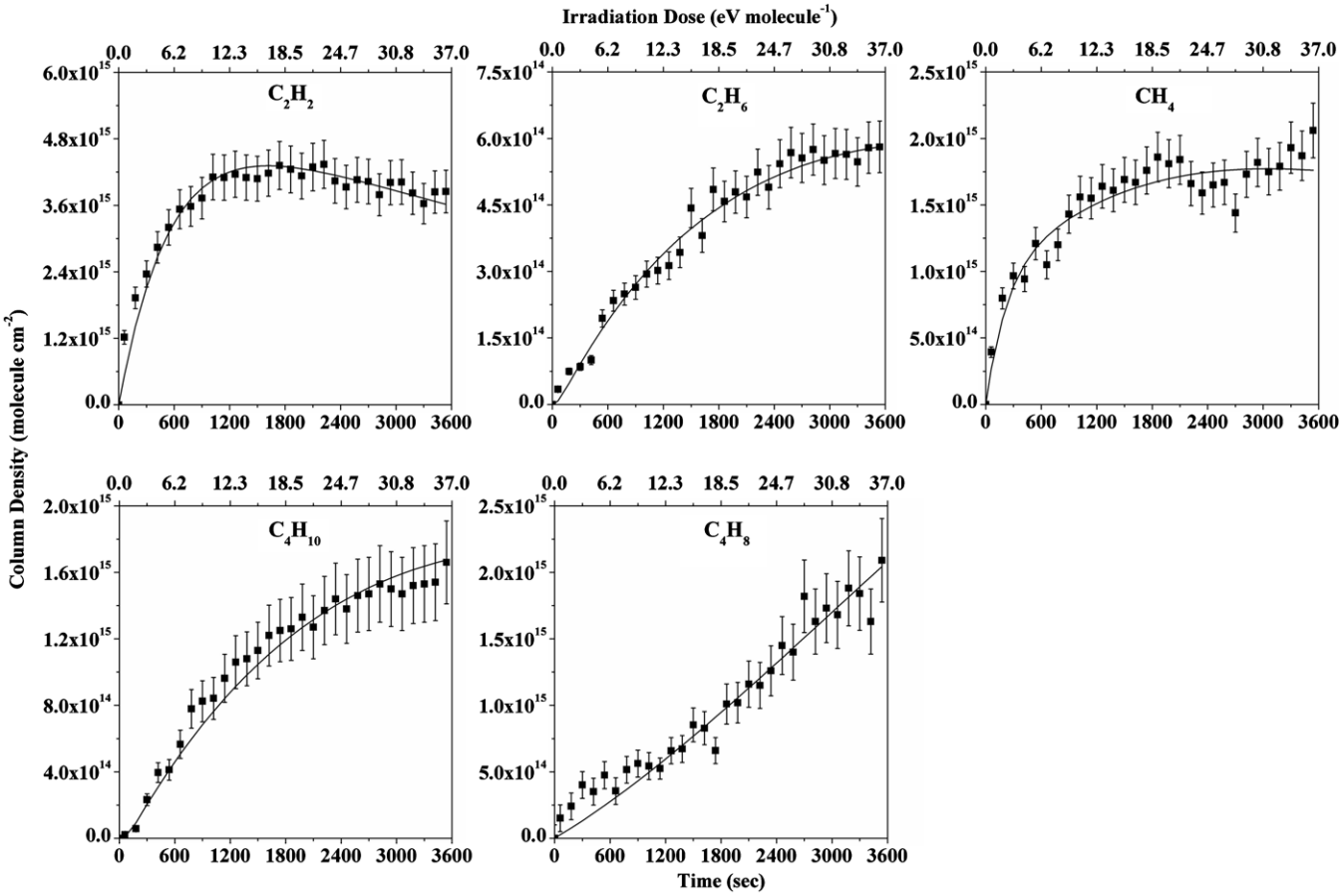

Figure 5. Column densities of acetylene (C_2H_2), ethane (C_2H_6), methane (CH_4), n-butane (C_4H_{10}), and 1-butene (C_4H_8) together with the derived fits.

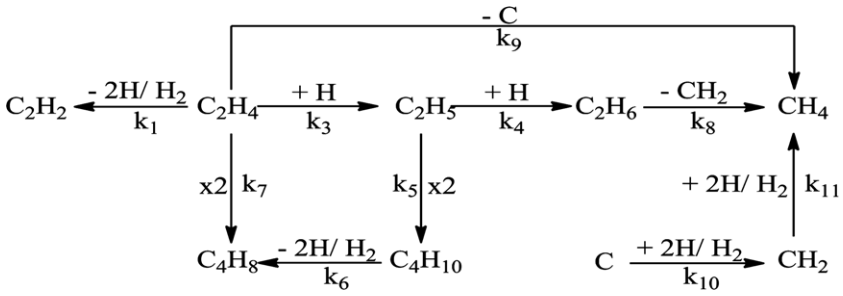

Figure 6. Reaction scheme used to fit the column densities as depicted in Figure 5.

dimerization of two ethylene molecules ($k_7 = 1.3 \pm 0.2 \times 10^{-25}$ cm^2 molecule^{-1} s^{-1}). Note that this reaction cannot happen between two closed-shell singlet reactants on the ground state surface. Considering the molecular structure of 1-butene ($H_2CCHCH_2CH_3$), this reaction might proceed via initial formation of singlet methylcarbene ($HCCH_3$) via [1, 2]-hydrogen migration, which then inserts with the carbine carbon atom into the carbon–hydrogen bond of a second ethylene molecule. Here singlet methylcarbene (CH_3CH; X^1A') is 3.06 eV higher in energy than ethylene (C_2H_4) and can be formed via hydrogen migration in singlet ethylene via a transition state ranging 3.27 eV above ethylene (Leonori et al. 2013; Nguyen et al. 2008). Triplet methylcarbene (CH_3CH; a^3A'') can be accessed via hydrogen migration in triplet ethylene (C_2H_4; a^3A_1). Here triplet ethylene (C_2H_4; a^3A_1) and triplet methylcarbene (CH_3CH; a^3A'') are 2.98 eV and 2.90 eV, respectively, higher in energy than ground state ethylene. Secondly, the transition state from triplet ethylene (C_2H_4; a^3A_1) to triplet methylcarbene (CH_3CH; a^3A'') is located 3.13 eV above ethylene (C_2H_4, a^1A_g; Leonori et al. 2013; Nguyen et al. 2008). It is important to stress that the proposed reaction scheme leads to an overproduction of acetylene (C_2H_2) and methane (CH_4), and destruction pathways of these molecules to hitherto unknown individual species—possibly to the polymeric residue—had to be incorporated ($k_2 = 3.8 \pm 0.5 \times 10^{-4}$ s^{-1}; $k_{12} = 3.2 \pm 0.4 \times 10^{-6}$ s^{-1}). The existence of a polymeric residue after the warming up of the irradiated sample is also supported by the carbon budget. As derived from the diminishing ethylene absorptions, during the electron exposure, $2.3 \pm 0.2 \times 10^{16}$ molecules cm^2 of ethylene were destroyed. Adding up the column densities of the newly formed C1, C2, and C4 molecules (Figure 5), only $1.2 \pm 0.3 \times 10^{16}$ molecules cm^2, i.e., 53% ± 20%, of the ethylene molecules are accounted for, suggesting that the remaining fraction is locked up in unidentified higher order products.

We would like to briefly address the application of the laboratory data to the modeling community. The irradiation experiments are conducted at averaged doses of 37 eV per molecule over 3600 s (1 hr) irradiation time. Therefore, the conversion factor (f) of $f(1000\ \text{nA}) = 10.4 \times 10^{-3}$ eV s^{-1} can be applied to transfer from the time domain to the actual energy deposition within the ethylene ices. This can be also expanded to the rate constant k. Here the units of the rate constant k are calculated—as mandatory for the kinetics community—and are given in s^{-1} for the formal unimolecular decomposition induced by energetic electrons. Here the division of the rate constant k in units of molecules s^{-1} by the conversion factor f in units of eV s^{-1} results in the numbers of molecules produced by eV absorbed inside the ices.

Finally, we would like to address briefly the underlying energetics associated in the radiolysis of the ethylene ices. The decomposition of ethylene (C_2H_4) to acetylene (C_2H_2) via two hydrogen atoms (2H) and/or molecular hydrogen (H_2) elimination requires 6.15 eV and/or 1.60 eV in energy (Kim et al. 2010). Considering the 11 K surrounding ice, this energy cannot be supplied thermally but is transferred by the impinging electrons to the target molecules via *nonequilibrium chemistry*. The competing hydrogen atom addition to ethylene (C_2H_4) leading to the formation of the ethyl radical (C_2H_5) is exoergic by 1.53 eV but has to pass a barrier of 0.10 eV (Kim et al. 2010). Once again, thermal chemistry cannot account for this pathway, and nonequilibrium processes possibly involving ethylene dimers are involved. Furthermore, the ethyl radical (C_2H_5) reaction with a hydrogen atom is barrier-less and exoergic (C_2H_6; −4.36 eV). The self-recombination of two ethyl radicals leads to n-butane (C_4H_{10}; −3.77 eV; Kim et al. 2010). Note that the radiolysis of n-butane (C_4H_{10}) to 1-butene (C_4H_8) via elimination of molecular hydrogen (H_2) and/or two hydrogen atoms is endoergic by 1.30 eV and 5.82 eV (Kim et al. 2010). Also, 1-butene can be formed via dimerization of two ethylene molecules in an overall exoergic pathway (1.08 eV). On the other hand, the radiolysis of ethane (C_2H_6) to methane (CH_4) and singlet carbene (CH_2) requires 4.32 eV (Kim et al. 2010); carbene can be hydrogenated to methane (−9.33 eV/−4.73 eV; Bennett et al. 2006).

It is important to place the present experiments in context. For this, we are comparing our results with previous experiments concerning the irradiation of ethylene ices. Kaiser & Roessler (1998) prepared ethylene ices at 10 K and studied their exposure to 9.0 MeV α-particles and 7.3 MeV protons in an ultrahigh vacuum chamber at a few 10^{-10} torr. The infrared spectra provide evidence of the formation of three C2 species: ethane (C_2H_6), acetylene (C_2H_2), and the ethyl radical (C_2H_5). Subsequently, Strazzulla et al. (2002) processed frozen ethylene at 12 K with 30 keV He^+ and 15 keV N^+. This work detected the formation of simple closed-shell C1 and C2 hydrocarbons: methane (CH_4), ethane (C_2H_6), and acetylene (C_2H_2)—but no radical intermediates. Compagnini et al. (2009) recorded Raman spectra to monitor the irradiation effects on 2 μm thick ethylene film at 16 K by 200 keV protons. The authors only identified one molecule: acetylene (C_2H_2). Finally, Ennis et al. (2011) bombarded solid ethylene at 10 K with 5 keV oxygen ions (O^+). Ennis et al. identified acetylene (C_2H_2) as an irradiation product via its ν_3 stretching mode at 3236 cm^{-1}. However, compared with previous works and the assignment of C1 (methane) and C2 hydrocarbons (ethane, ethyl radical, acetylene), the present investigation provides the very first evidence that the radiation processing of ethylene ices can also lead to two prominent C4 hydrocarbons: 1-butene (C_4H_8) and n-butane (C_4H_{10}), which were not reported previously.

5. ASTROPHYSICAL IMPLICATIONS

It is important to place these experimental findings into a broader context. C1 and C2 hydrocarbons are common constituents of ices in the outer solar system and in the interstellar medium (ISM). In our solar system, there is evidence for areas of pure methane on the surfaces of Pluto (Douté et al. 1999), Eris (Merlin et al. 2009), and Quaoar (Brown 2012) with variations of millimeter size grains to large portions of pure methane covering Pluto's surface. In the atmosphere of Uranus and Neptune (Samuelson 1998), methane-based ice clouds are also believed to be present. Ethane is possibly on Pluto (Barucci et al. 2008b) and Orcus (Barucci et al. 2008b; Delsanti et al. 2010). Furthermore, ethane has been detected on the surfaces of Makemake (Brown et al. 2007), Quaoar (Schaller & Brown 2007), and KBO 1993SC, with the evidence for 1993SC and Quaoar implying hitherto unidentified *higher order hydrocarbons* to be present as well (Brown et al. 1997). Finally, ethane is also of potential relevance to Saturn's moon Titan in the form of solid ethane ice droplets (Lang et al. 2011). In 2009, Bauerecker & Dartois (2009) simulated the growth of ethane aerosols in the laboratory, demonstrating that gaseous ethane condenses first in its liquid phase and then grows to micrometer-sized droplets accompanied by morphological changes toward crystalline solids. Hunten (2006) pointed out that ethane is possibly seeding the cloud formation in the cold atmosphere of Titan and gradually depositing solid ethane droplets on Titan's surface. The confirmation of ethane in Titan's atmosphere has actually been achieved via mass spectroscopy at the Huygens landing site (Niemann et al. 2005). Also, note that to interpret the reflection data of the Cassini images, scientists propose the existence of hydrocarbon-based ethane lakes on the surface of Titan such as Ontario Lacus (Brown et al. 2008).

In the ISM, interstellar grains have been found to be coated with an icy "mantle" consisting mainly of water (H_2O) followed by methanol (CH_3OH), carbon monoxide (CO), carbon dioxide (CO_2), methane (CH_4), ammonia (NH_3), and formaldehyde (H_2CO) with thicknesses of up to a few hundred nanometers (Ehrenfreund & Schutte 2000; Gibb et al. 2000, 2004). The interaction of these ices with GCRs and with the internal ultraviolet field inside cold molecular clouds has repeatedly been demonstrated to chemically modify the pristine ices via nonthermal, nonequilibrium chemistry involving suprathermal reactants such as hydrogen, oxygen, nitrogen, and carbon atoms (Kaiser et al. 1997; Bennett & Kaiser 2007, Bennett et al. 2005; Zheng & Kaiser 2007). Therefore, in cold molecular clouds, the interaction of ionizing radiation with ice-coated nanoparticles is expected to lead to the synthesis of complex organic molecules, which cannot be explained by classical thermal reactions. Once the molecular cloud collapses and transforms to star-forming regions, the elevated temperatures of up to about 250 K result in a sublimation of these newly formed organic molecules, which are then monitored by radio astronomy. Note that methane (CH_4) has been observed in 18 out of 23 young stellar objects by the *Infrared Space Observatory* at levels of typically 1%–5%. The C2 hydrocarbons acetylene, ethylene, and ethane have not been detected on interstellar ices yet but can be formed upon radiolysis of methane ices (Kaiser & Roessler 1997).

An understanding of the radiation-induced chemistry of C1 and C2 species as observed in extraterrestrial low temperature ices is crucial to rationalize the hydrocarbon balance in the outer

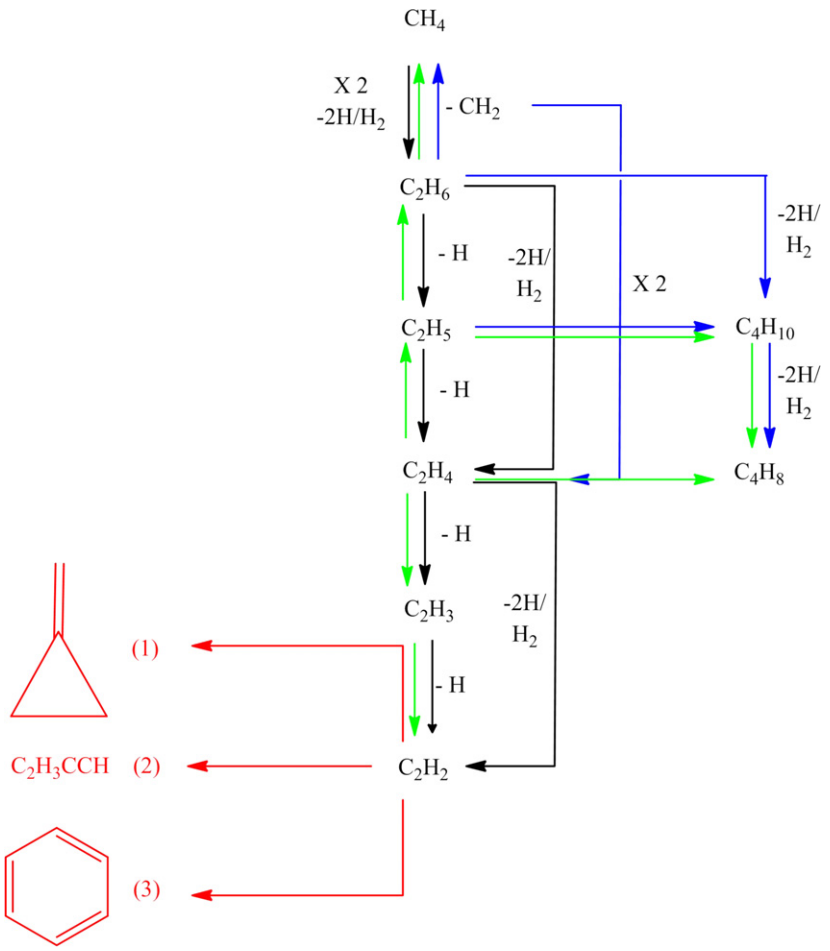

Figure 7. Comparison of the radiation products and underlying pathways formed in ices of C1 (methane; black) and C2 (ethane (blue), ethylene (green), acetylene (red)) ices upon interaction of energetic electrons at 11 K.

(A color version of this figure is available in the online journal.)

solar system and in the ISM (Figure 7). First, starting from methane, Bennett et al. (2006) and Kaiser & Roessler (1998) provided evidence that the C2 hydrocarbons ethane (C_2H_6), ethylene (C_2H_4), and acetylene (C_2H_2) together with their radical intermediates ethyl (C_2H_5) and vinyl (C_2H_3) can be formed sequentially and—in case of ethylene (C_2H_4) and acetylene (C_2H_2)—via dehydrogenation from ethane (C_2H_6). Kim et al. (2010) provided evidence that in irradiated ethane ices (C_2H_6), the latter can be also effectively converted to ethylene (C_2H_4) and acetylene (C_2H_2); likewise, the present studies conclude that ethylene (C_2H_4) can be easily converted to acetylene (C_2H_2) and ethane (C_2H_6) via dehydrogenation and hydrogenation, respectively. Therefore, it is evident that the C2 hydrocarbons can be linked to each other with the actual concentration dictated by the hydrogen concentration in the system, i.e., hydrogen-rich versus hydrogen-poor.

Further studies have been conducted on the processing of methane ice with a variety of energetic particles, including high-energy ions (Kaiser & Roessler 1997, 1998; Moore & Hudson 2003; de Barros et al. 2011; Baratta et al. 2002, 2003; Ferini et al. 2004; Brunetto et al. 2006; Lecluse et al. 1998), high- and low-energy electrons (Jones & Kaiser 2013; Bennett et al. 2006; Huels et al. 2008; Barberio et al. 2013), broad band UV photons (Moore & Hudson 2003; Baratta et al. 2002; Gerakines et al. 1996), and γ radiation (Davis & Libby 1964; Davis et al. 1966). The bombarded ices were mainly analyzed by FTIR spectroscopy identifying acetylene (C_2H_2), ethylene (C_2H_4), ethane (C_2H_6), and propane (C_3H_8) as products. However, a recent study conducted in our group (Jones & Kaiser 2013) demonstrated that complex hydrocarbons (*up to* $C_{22}H_n$) are formed at doses well below the total accumulated dose (165 eV molecule^{-1}) within the surface of Pluto (Johnson 1989). This result is in agreement with a previous study on the photolysis of methane with broadband UV light, which identified a "high order volatile," but could only speculate the volatile to contain C_2–C_7 hydrocarbons (Gerakines et al. 1996). In addition, vibrational modes characteristic of di- and tri-substituted benzenes were observed in the MeV proton and α-particle irradiation of methane ice (Kaiser & Roessler 1997), suggesting the presence of the PAHs naphthalene, phenanthrene, and anthracene. Furthermore, this study was the only one to monitor the products as they sublimed into the gas phase. Thus far, only one study utilized Raman spectroscopy to examine the effects on the organics synthesized within the ion irradiation of methane ice. The energy dose was quite extensive (1000 eV molecule^{-1}), and only a broad peak was observed corresponding to C = C stretching of amorphous carbon. The ultraviolet–visible reflectance upon the irradiation of methane was investigated; unfortunately, this only focused on the reflectance curve and the relationship of this to colors of Centaurs and Trans-Neptunian objects—no products were identified (Baratta et al. 2008). Recently, the temperature program desorption studies (Barberio et al. 2013) on high energy electron irradiation of methane ice revealed that ethane and acetylene are formed.

Besides the C2 hydrocarbons, our studies predict that in ethane-, ethylene-, and acetylene-bearing solar system and interstellar ices, an interaction of ionizing radiation can also lead to C4 and C6 hydrocarbons (Figure 7). Depending on the hydrocarbon content, hydrogen-rich ices (ethane, ethylene) also result in the formation of n-butane (C_4H_{10}) together with 1-butene (C_4H_8). In hydrogen-poor ices (acetylene), both vinylacetylene (C_4H_4) and its methylenecyclopropene isomer (C_4H_4) together with benzene (C_6H_6) were formed. To our knowledge, these species have not been incorporated into any ice models simulating the chemical evolution of outer solar system or interstellar hydrocarbon-rich ices. This is particularly true for Titan's surface chemistry as GCRs have been known to penetrate deep into the atmosphere and ultimately generating cascades of secondary particle, which can then build up higher molecular mass hydrocarbons from their C1 and C2 precursors. Finally, we should point out that higher order hydrocarbons such as 1-butene and n-butane in this work have the potential to be "building blocks" for "organic" sand dunes observed by Cassini for Titan (Radebaugh et al. 2008). Recently, Jones & Kaiser (2013) applied reflectron time-of-flight mass spectrometry coupled to soft photoionization to study the radiation-induced processes in methane ices at temperatures as low as 5 K. The results show that complex hydrocarbons with up to C22 can be formed in electron-irradiated methane ices, including alkanes, alkenes, and alkyne/dienes, with the later classes identified for the first time. These studies are particularly timely since they will provide solid laboratory data that can be compared with data from the New Horizons mission to Pluto to eventually reveal a better understanding of the formation of our solar system.

Finally, we would like to highlight that it is imperative to conduct simulation experiments of the interaction of GCR particles and their secondary electrons with frozen ices found in the ISM and in the outer solar system. However, these experiments can never simulate the complexity of extraterrestrial environments such as a wide range of kinetic energies of the irradiating particles and the UV irradiation field as well as the composition of the ice targets themselves. Here the laboratory experiments have to be designed so that an understanding of the physical and chemical processes, including the formation of new molecules, is based on simulation experiments involving relatively simple model systems such as ethane (Kim et al. 2010), ethylene, and acetylene (Zhou et al. 2010) ices under controlled circumstances before expanding the simulation experiments to more complex systems. The derived reaction mechanisms, however, on the hydrocarbon ices present versatile pathways to form more complex hydrocarbons in these low temperature environments and can be transferred without restrictions to extraterrestrial ices. Since the investigation of the pure model ices have been completed, the next step would be to investigate the interaction of cosmic ray particles and their secondary electrons with a realistic mixture of hydrocarbon ices.

The work was supported by the Chemistry Division of the U.S. National Science Foundation within the framework of the Collaborative Research in Chemistry (CRC) Program (NSF-CRC CHE-0627854).

REFERENCES

Baratta, G. A., Brunetto, R., Leto, G., et al. 2008, JRSp, 39, 211
Baratta, G. A., Domingo, M., Ferini, G., et al. 2003, NIMPB, 209, 283
Baratta, G. A., Leto, G., & Palumbo, M. E. 2002, A&A, 384, 343
Barberio, M., Vasta, R., Barone, P., Manico, G., & Xu, F. 2013, WJCMP, 3, 14
Barucci, M. A., Brown, M. E., Emery, J. P., et al. 2008a, in The Solar System Beyond Neptune, Composition and Surface Properties of Transneptunian Objects and Centaurs, ed. M. A. Barucci, H. Boehnhardt, D. P. Cruikshank, A. Morbidelli, & Renee Dotson (Tucson, AZ: Univ. Arizona Press), 143
Barucci, M. A., Merlin, F., Guilbert, A., et al. 2008b, A&A, 479, L13
Bauerecker, S., & Dartois, E. 2009, Icar, 199, 564
Bennett, C. J., Jamieson, C. S., Mebel, A. M., & Kaiser, R. I. 2004, PCCP, 6, 735
Bennett, C. J., Jamieson, C. S., Osamura, Y., & Kaiser, R. I. 2006, ApJ, 653, 792
Bennett, C. J., Jamieson, C. S., Osamura, Y., et al. 2005, ApJ, 624, 1097
Bennett, C. J., & Kaiser, R. I. 2007, ApJ, 661, 899
Brecher, C., & Halford, R. S. 1961, JChPh, 35, 1109
Brown, M. E. 2012, AREPS, 40, 467
Brown, M. E., Barkume, K. M., Blake, G. A., et al. 2007, AJ, 133, 284
Brown, R. H., Cruikshank, D. P., Pendleton, Y., & Veeder, G. 1997, Sci, 276, 937
Brown, R. H., Soderblom, L. A., Soderblom, J. M., et al. 2008, Natur, 454, 607
Brunetto, R., Barucci, M. A., Dotto, E., & Strazzulla, G. 2006, ApJ, 644, 646
Comeford, J. J., & Gould, J. H. 1960, JMoSp, 5, 474
Compagnini, G., D'Urso, L., Puglisi, O., Baratta, G. A., & Strazzulla, G. 2009, Carbon, 47, 1605
Coustenis, A., Achterberg, R. K., Conrath, B., et al. 2007, Icar, 189, 35
Coustenis, A., Salama, A., Schulz, B., et al. 2003, Icar, 161, 383
Coustenis, A., Schmitt, B., Khanna, R., & Trotta, F. 1999, P&SS, 47, 1305
Dangi, B. B., Parker, D. S. N., Kaiser, R. I., Jamal, A., & Mebel, A. M. 2013, Angew. Chem., Int. Ed. Engl., 52, 7186
Davis, D. R., & Libby, W. F. 1964, Sci, 144, 991
Davis, D. R., Libby, W. F., & Meinschein, W. G. 1966, JChPh, 45, 4481
de Barros, A.L.F., Bordalo, V., Duarte, E., et al. 2011, A&A, 531, A160
Delsanti, A., Merlin, F., Bauer, J., et al. 2010, A&A, 520, A40
Douté, S., Schmitt, B., Quirico, E., et al. 1999, Icar, 142, 421
Drouin, D., Couture, A. R., Gauvin, R., et al. 2001, Monte Carlo Simulation of Electron Trajectory in Solids (CASINO Ver. 2.42; Sherbrooke: Univ. Sherbrooke)
Ehrenfreund, P., & Schutte, W. A. 2000, in IAU Symp. 197, Astrochemistry: From Molecular Clouds to Planetary Systems, ed. Y. C. Minh & E. F. van Dishoeck (San Francisco, CA: ASP), 135
Ennis, C., Yuan, H. Q., Sibener, S. J., & Kaiser, R. I. 2011, PCCP, 13, 17870
Ferini, G., Baratta, G. A., & Palumbo, M. E. 2004, A&A, 414, 757
Gerakines, P. A., Schutte, W. A., & Ehrenfreund, P. 1996, A&A, 312, 289
Gibb, E. L., Nummelin, A., Irvine, W. M., Whittet, D. C. B., & Bergman, P. 2000, ApJ, 545, 309
Gibb, E. L., Whittet, D. C. B., Boogert, A. C. A., & Tielens, A. G. G. M. 2004, ApJ, 151, 35
Gu, X., Kim, Y. S., Kaiser, R. I., et al. 2009, PNAS, 106, 16078
Heavens, O. S. 1965, in Optical Properties of Thin Solid Films (New York: Dover), 114
Huang, C., Zhang, F., Kaiser, R. I., et al. 2010, ApJ, 714, 1249
Huels, M. A., Parenteau, L., Bass, A. D., & Sanche, L. 2008, IJMSp, 277, 256
Hunten, D. M. 2006, Natur, 443, 669
Johnson, R. E. 1989, GeoRL, 16, 1233
Jones, B. M., & Kaiser, R. I. 2013, J. Phys. Chem. Lett., 4, 1965
Jones, B. M., Zhang, F., Kaiser, R. I., et al. 2011, PNAS, 108, 452
Kaiser, R. I., Eich, G., Gabrysch, A., & Roessler, K. 1997, ApJ, 484, 487
Kaiser, R. I., & Mebel, A. M. 2012, Chem. Soc. Rev., 41, 5490
Kaiser, R. I., Parker, D. S. N., Zhang, F., et al. 2012, JPCA, 116, 4248
Kaiser, R. I., & Roessler, K. 1997, ApJ, 475, 144
Kaiser, R. I., & Roessler, K. 1998, ApJ, 503, 959
Kim, Y. S., Bennett, C. J., Chen, L.-H., O'Brien, K., & Kaiser, R. I. 2010, ApJ, 711, 744
Lang, E. K., Knox, K. J., Wang, C.-C., & Signorell, R. 2011, P&SS, 59, 722
Lecluse, C., Robert, F., Kaiser, R. I., et al. 1998, A&A, 330, 1175
Leonori, F., Skouteris, D., Petrucci, R., et al. 2013, JChPh, 138, 024311
Lunine, J. I., & Lorenz, R. D. 2009, AREPS, 37, 299
Merlin, F., Alvarez-Candal, A., Delsanti, A., et al. 2009, AJ, 137, 315
Molina-Cuberos, G. J., López-Moreno, J. J., Rodrigo, R., Lara, L. M., & O'Brien, K. 1999, P&SS, 47, 1347
Moore, M. H., & Hudson, R. L. 2003, Icar, 161, 486
Nguyen, M. T., Matus, M. H., Lester, W. A., Jr., & Dixon, D. A. 2008, JPCA, 112, 2082
Niemann, H. B., Atreya, S. K., Bauer, S. J., et al. 2005, Natur, 438, 779
Pacansky, J., & Schrader, B. 1983, JChPh, 78, 1033
Parker, D., Zhang, F., Kaiser, R. I., et al. 2012, PNAS, 109, 53
Radebaugh, J., Lorenz, R. D., Luninec, J. I., et al. 2008, Icar, 194, 690
Raulin, F. 2005, SSRv, 116, 471

Sagan, C., & Thompson, W. R. 1984, Icar, 59, 133
Samuelson, R. 1998, in Solar System Ices: Atmospheric Ices, ed. B. Schmitt, C. de Bergh, & M. Festou (The Netherlands: Kluwer), 767
Schaller, E. L., & Brown, M. E. 2007, ApJL, 670, L49
Sigurbjornsson, O. F., & Signorell, R. 2008, PCCP, 10, 6211
Strazzulla, G., Baratta, G. A., Domingo, M., & Satorre, M. A. 2002, NIMPB, 191, 714
Tomasko, M. G., Doose, L. R., Dafoe, L. E., & See, C. 2009, Icar, 204, 271
Vinatier, S., Bezard, B., Fouchet, T., et al. 2007, Icar, 188, 120
Zhang, F., Kim, S., Kaiser, R. I., Krishtal, S. P., & Mebel, A. M. 2009a, JPCA, 113, 11167
Zhang, F., Kim, S., Kaiser, R. I., & Mebel, A. M. 2009b, JChPh, 130, 234308
Zheng, W. J., & Kaiser, R. I. 2007, CPL, 450, 55
Zhou, L., Kaiser, R. I., Gao, L. G., et al. 2008, ApJ, 686, 1493
Zhou, L., Zheng, W., Kaiser, R. I., et al. 2010, ApJ, 718, 1243